

# Blue Light Switchable Cell–Cell Interactions Provide Reversible and Spatiotemporal Control Towards Bottom-Up Tissue Engineering

Simge G. Yüz, Samaneh Rasoulinejad, Marc Mueller, Anatol E. Wegner, and Seraphine V. Wegner\*

Controlling cell–cell interactions is central for understanding key cellular processes and bottom-up tissue assembly from single cells. The challenge is to control cell–cell interactions dynamically and reversibly with high spatiotemporal precision noninvasively and sustainably. In this study, cell–cell interactions are controlled with visible light using an optogenetic approach by expressing the blue light switchable proteins CRY2 or CIBN on the surfaces of cells. CRY2 and CIBN expressing cells form specific heterophilic interactions under blue light providing precise control in space and time. Further, these interactions are reversible in the dark and can be repeatedly and dynamically switched on and off. Unlike previous approaches, these genetically encoded proteins allow for long-term expression of the interaction domains and respond to nontoxic low intensity blue light. In addition, these interactions are suitable to assemble cells into 3D multicellular architectures. Overall, this approach captures the dynamic and reversible nature of cell–cell interactions and controls them noninvasively and sustainably both in space and time. This provides a new way of studying cell–cell interactions and assembling cellular building blocks into tissues with unmatched flexibility.

It is the vision of bottom-up tissue engineering to assemble cellular building blocks into multicellular functional tissues. This requires precisely controlling the interactions between the cells in space and time to obtain multicellular architectures that match the complexity of natural tissues.<sup>[1]</sup> In fact cell–cell interactions play a crucial role not only in maintaining tissue integrity, but also in how cells organize with respect to each

other, work together, and regulate cell behavior through associated intracellular signaling (motility, collective migration, differentiation, etc.).<sup>[2]</sup> In general cell–cell interactions and the associated signaling are very dynamic while being spatially and temporally tightly regulated during important events such as embryogenesis, wound healing, and cancer progression.<sup>[3]</sup> It is this tight regulation of cell–cell interactions and signals that is in part responsible for the proper development of tissues and organs at the right time in the right place<sup>[4]</sup> and their dysregulation is involved in cancer cells leaving the primary tumor and metastasizing in other organs.<sup>[5]</sup> Clearly, the ability to regulate cell–cell interactions dynamically and with high spatiotemporal control is a key to assembling cellular building blocks into predictable tissue structures in the context of bottom-up tissue engineering, as well as to understanding and manipu-

lating biological processes where cell–cell interactions play a pivotal role.

The fabrication of precisely controlled biomimetic materials has provided us with a detailed picture of cell–matrix interactions allowing us to design scaffolding materials for regenerative medicine.<sup>[6]</sup> However, our ability to control cell–cell interactions with high spatial and temporal precision lags behind this development. The main difficulty is that, in contrast to synthetic materials, it is far from straightforward to modify the surface of the cell directly and sustainably in a way that will provide control in space and time. In recent years, chemical modification of cell surfaces with bioorthogonal functional groups has become an attractive way to control cell–cell interactions. Bioorthogonal functional groups (e.g., azides-alkynes,<sup>[7]</sup> oxyamines-ketones<sup>[8]</sup>), or strong noncovalent interaction partners<sup>[9]</sup> (e.g., complementary DNA strands,<sup>[10]</sup> biotin-avidin<sup>[11]</sup>), have been introduced to the cell surface through liposome fusion or modified sugars<sup>[12]</sup> to induce specific interactions between cells with complementary reactive groups. However, unlike natural cell–cell interactions, these interactions are neither reversible nor dynamic. While DNA based cell assemblies can be reversed using degrading enzymes, increased temperatures, and displacing stands, these methods are either invasive

Dr. S. G. Yüz, S. Rasoulinejad, M. Mueller, Dr. S. V. Wegner  
Max Planck Institute for Polymer Research  
Ackermannweg 10, 55128 Mainz, Germany  
E-mail: wegner@mpip-mainz.mpg.de

Dr. S. G. Yüz  
Department of Biophysical Chemistry  
University of Heidelberg  
Im Neuenheimer Feld 253, 69120 Heidelberg, Germany

Dr. A. E. Wegner  
Department of Statistical Science  
University College London  
Gower Street, London WC1E 6BT, UK

 The ORCID identification number(s) for the author(s) of this article can be found under <https://doi.org/10.1002/adbi.201800310>.

DOI: 10.1002/adbi.201800310

or irreversible.<sup>[10]</sup> Only the surface modification of cells with lipid-chemically self-assembled nanorings allows to reversibly induce cell–cell interactions.<sup>[9]</sup> Another limitation is that chemical modifications to the cell surface can interfere unpredictably with other biological processes. Notably, such unnatural modifications only physically bring cells into proximity but do not directly communicate the signals associated to natural cell–cell interactions and only indirectly lead to cellular responses.<sup>[7,8,10c]</sup> Additionally, chemical modifications are difficult to sustain over longer periods since they are not embedded in any cellular machinery, and will diminish as cells divide and degrade them. Most importantly, these chemical modifications do not provide high spatial or temporal control over the cell–cell interactions.

Recently, light responsive chemical groups have been introduced to the cell surface to gain better spatiotemporal control over cell–cell interactions. For example, cell–cell interactions that were mediated by a linker with a nitrobenzene group can be locally disrupted when illuminated with UV light.<sup>[13]</sup> Similarly, the photoswitchable binding between azobenzene and cyclodextrin has been integrated on the cell surface to provide the first reversible switching of cell–cell interactions with light and have been used to study cell–cell communication.<sup>[14]</sup> On the down side, however, all of these interactions respond to UV light, which is toxic for cells and the general problems associated with the chemical modification of cell surfaces still hold true. Genetically encoded cell–cell interactions are an alternative to chemical modifications on the cell surface.<sup>[2c]</sup> These are sustained over time and are biocompatible, but it is problematic—if not impossible—to alter these cell–cell interactions locally and rapidly. Overall, a platform is still missing in order to control cell–cell interactions dynamically, reversibly, and with high spatial and temporal resolution in a noninvasive, sustainable, and bio-orthogonal way. Clearly, the design and development of photoswitchable cell–cell interactions that fulfill these requirements would enable us to study cell–cell interactions and to buildup complex multicellular architectures.

Herein, we developed blue light switchable cell–cell interactions, which can overcome all the above-listed limitations. We express the protein CRY2 (cryptochrome 2) and its interaction partner, CIBN (N-terminal of Cry-interacting basic helix-loop-helix protein 1) on the surfaces of cells, as photoswitchable building blocks to mediate cell–cell interactions. CRY2 and CIBN bind to each other upon blue light (480 nm) illumination and reversibly dissociate in the dark within minutes.<sup>[15]</sup> Using the blue light-dependent heterodimerization of CRY2 and CIBN provide us with the desired high spatial and temporal control and offer us an interactions that is both dynamic and reversible.<sup>[16]</sup> The CRY2/CIBN interaction has already been used to control a variety of intracellular functions (e.g., gene transcription,<sup>[17]</sup> protein–protein interactions,<sup>[18]</sup> cell signaling,<sup>[19]</sup> organelle distribution,<sup>[20]</sup> mechanotransduction<sup>[21]</sup>) and cell adhesion to substrates,<sup>[22]</sup> which also shows the high bioorthogonality of the CRY2/CIBN interaction. This interaction is induced by using low intensities of visible blue light, making this optogenetic approach noninvasive. The fact that these proteins are genetically encoded provides us with sustainable expression of these proteins on the cell surface over time. Like other examples to control cell–cell interactions, we use the

CRY2/CIBN protein pair to control the interactions but not the signaling associated to cell–cell interactions.

To attain blue-light dependent cell–cell interactions, we expressed CRY2 and CIBN on the surfaces of MDA-MB-231 cells, which lack E-cadherin expression and do not form any native cell–cell contacts.<sup>[23]</sup> We hypothesized that upon blue-light illumination those cells expressing the complementary interaction partners CRY2 and CIBN would interact and form cell clusters (Figure 1A). To express these proteins on the cell surface, we inserted CRY2-mCherry and CIBN-GFP (green fluorescent protein) into a pDisplay plasmid with an N-terminal Ig  $\kappa$ -chain leader sequence to direct the protein to the secretory pathway and a C-terminal transmembrane domain of the PDGFR (platelet derived growth factor receptor) for anchoring in the cell membrane. Subsequently, we transfected MDA-MB-231 cells with one of these plasmids and generated the stable cell lines, CRY2-MDA and CIBN-MDA, which constantly express the respective protein on the cell surface. Immunostainings of unpermeabilized cells for c-myc epitope, also included in the extracellular part of the displayed proteins, and fluorescence images of the fused fluorescent proteins show that the proteins are expressed and displayed on the cell surface (Figures S1 and S2, Supporting Information). Yet, attempts to quantify the protein expression levels in these cells with western blot, flow cytometry, and mass spectroscopy failed, presumably due to low protein expression. Nonetheless, we explored if the displayed CRY2 and CIBN proteins can mediate blue light dependent cell–cell interactions.

Cells grow as single cells in the absence of cell–cell interactions (e.g., MDA-MB-231 cells) but grow in clusters of cells if cell–cell interactions are strong like cells of epithelial types (e.g., MCF7 cells). In order to check if the CRY2 and CIBN expressing cells form cell–cell interactions under blue light, we mixed CRY2-MDA and CIBN-MDA cells in equal proportions and cocultured them on a glass substrate either in the dark or under blue light for 4 h. To better visualize the cell boundaries and their positions, we stained the actin cytoskeleton with phalloidin-tetramethylrhodamine and the nuclei with 4',6-diamidino-2-phenylindole (DAPI). In the dark, the mixed CRY2-MDA and CIBN-MDA cells grow as single cells similar to the parent MDA-MB-231 cells and have little interaction with neighboring cells as can be observed in fluorescent images (Figure 1B; Figure S3, Supporting Information). On the other hand, under blue light illumination the mixed cells grow in clusters and showed cell–cell contacts between neighboring cells. This finding already shows that the blue light-dependent interaction between CRY2 and CIBN is suitable to prompt cell–cell interactions.

To demonstrate that there is significantly more cell–cell interactions under blue light than in the dark we used two different methods; an analysis of cells that are in direct contact, i.e., growth in clusters and a statistical analysis of the cell positions' in space.

As mentioned above a direct consequence of strong cell–cell interactions is that the cells start to grow in clusters. To investigate blue light dependent cell–cell interactions, we quantified the number of cells that grow in clusters and as single cells in the dark and under blue light. For this purpose, we mixed CRY2-MDA and CIBN-MDA cells and cultured them in the dark or under blue light for 4 h during which they could form cell–cell

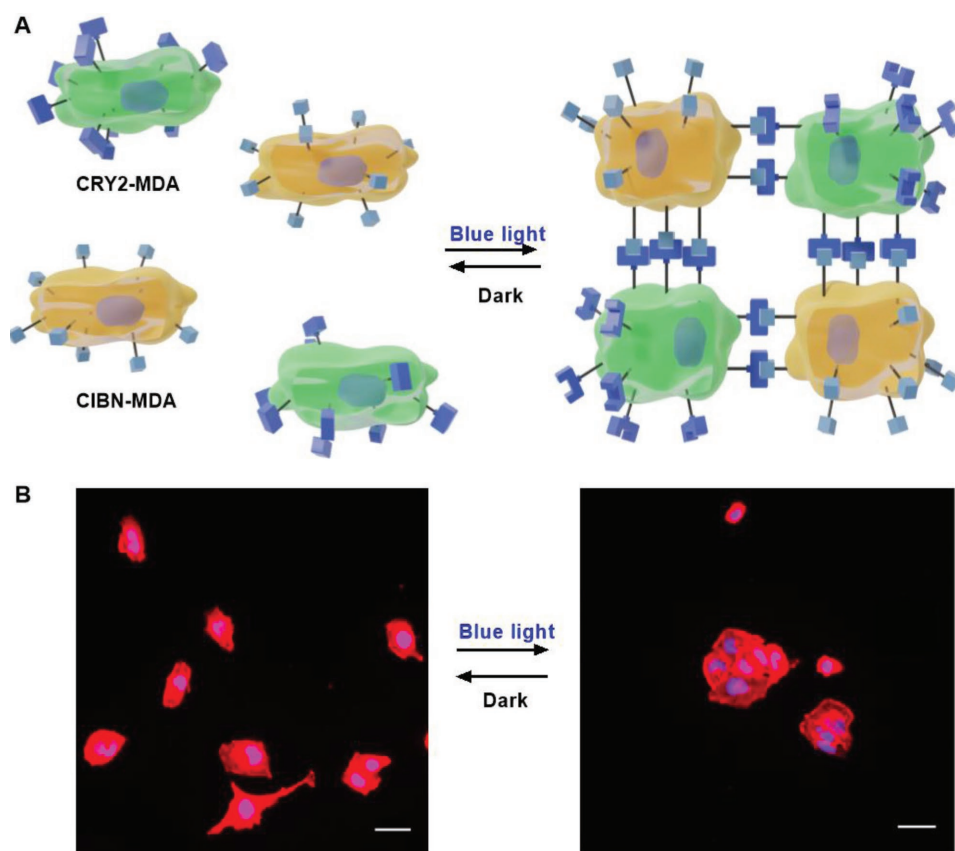


**Figure 1.** Blue-light switchable cell–cell interactions. A) Cells that express CRY2 (green) and CIBN (yellow) form cell–cell interactions under blue light and dissociate from each other in the dark. B) CRY2-MDA and CIBN-MDA cells are mixed in equal proportions and cultured in the dark or under blue light illumination. Cells cultured in the dark remain as single cells, but cells cultured under blue light form cell clusters due to CRY2-CIBN heterodimerization. Red: actin stain, Blue: nuclear stain. Scale bars are 50  $\mu\text{m}$ .

interactions and also adhere to a glass surface. First, we varied the overall cell density of cultured cells so that we could reliably observe light dependent cell–cell interactions. We determined the optimal density to be 5000 cells  $\text{cm}^{-2}$  ( $\approx 5\%$  confluency) since at higher cell densities the light dependent cell–cell interactions are not distinguishable from general crowding in the cell culture and at lower cell densities the cells are too sparse to efficiently find each other (Figure S4A,C, Supporting Information). To visualize cells in close proximity, which presumably form cell–cell interactions, we stained the actin cytoskeleton, acquired fluorescence images for a total area of 1  $\text{cm}^2$  ( $\approx 5000$  cells  $\text{cm}^{-2}$ , technical duplicates with two replicates each) and analyzed the spreading area for all objects in these images. The actin staining allowed us to distinguish single cells (spreading area, i.e., objects with an area of 300–3000  $\mu\text{m}^2$ ) from cell clusters that contain more than three cells (clusters of connected cells; objects with an area  $> 10\,000$   $\mu\text{m}^2$ ) since cells growing in a cluster have an at least three times larger combined spreading area than a single cell. (Objects with an area of 3000–10 000  $\mu\text{m}^2$  are not assigned in the clustering analysis as they contain 1–3 cells and it is difficult to classify them reliably as single cells or clusters.) In a 1:1 mixed coculture of CRY2-MDA and CIBN-MDA cells, we detected about 180 cell clusters  $\text{cm}^{-2}$  under blue light while there were only about 20 clusters  $\text{cm}^{-2}$

in the dark (Figure 2A). Conversely, in the same cultures the number of single cells was also significantly less under blue light compared to those in the dark. Likewise, the percent of area occupied by cell clusters compared to the area of all cells, which is proportional to the percentage of cells involved in cell clusters, is sixfold higher under blue light than in the dark (Figure 2B). In fact, under blue light about 30% of cells grow in clusters of cells that contain more than three cells and only 30% are growing as single cells, while in the dark about 70% are growing as single cells. All of these parameters demonstrate clearly that CRY2 and CIBN expressing cells interact more with each other under blue light than in the dark.

To make sure that the increase in cell clustering under blue light is not due to differences in cell seeding or light toxicity, we measured the total number of cells in each culture based on the nuclear DAPI stain. We found that there were no significant differences in the total number of cells between cultures (Figure S7, Supporting Information). Next, we verified that blue light illumination did not lead to toxicity. In the parent cell line (MDA-MB-231), we did not observe any phototoxicity even at 8000  $\mu\text{W cm}^{-2}$  after 4 h, which is 100-fold higher light intensity than we used in cell clustering experiments (Figure S5, Supporting Information). This also demonstrates that the light

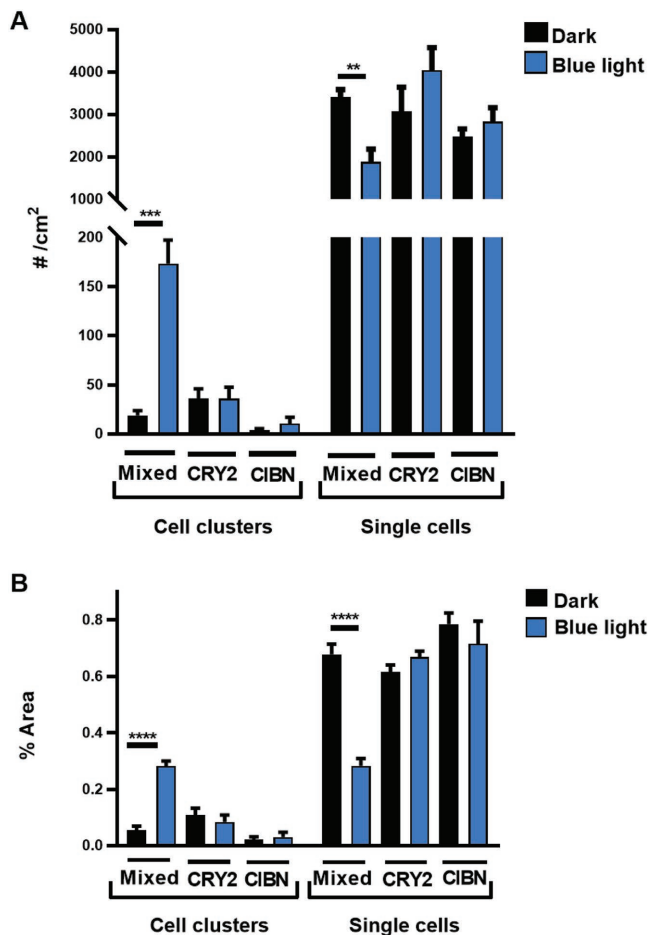


**Figure 2.** Quantification of cell–cell interactions between CRY2-MDA and CIBN-MDA cells in the dark and under blue light. A) The number of cell clusters > three cells and single cells in the dark and under blue light. B) Percentage of Area of cells that grow in cell clusters and as single cells. The cells kept in the dark mainly stay as single cells, whereas cells grown under blue light show a higher number of cell clusters. CRY2-MDA and CIBN-MDA cells form heterophilic and not homophilic interactions as cells in monocultures grow as single cells. The error bars are the standard error of technical duplicates with two replicates ( $n = 4$ ). Unpaired t-test is used for statistical significance ( $p$  value  $<0.01$  (\*\*),  $<0.001$  (\*\*\*),  $<0.0001$  (\*\*\*\*)).

intensities used here are far below the toxic dose, making this approach noninvasive for cells.

The Ripley's  $K$ -function<sup>[24]</sup> is a standard statistical measure to determine if points in space are clustered ( $K(r) > K_0(r)$ ), randomly distributed ( $K(r) = K_0(r)$ ) or dispersed ( $K(r) < K_0(r)$ ) compared to a random distribution of points ( $K_0$ ) at length scale  $r$ . In this study, we took the center of mass for each cell nucleus detected by DAPI staining as a point and analyzed if these points cluster more under blue light illumination compared to the dark. We use the variance stabilized transformation of Ripley's  $K$ -function known as the  $L$ -function. Indeed, the  $L$ -function analysis shows that there is significantly more clustering under blue light than in the dark, since  $L_{\text{blue}} > L_{\text{dark}}$  at distances of 10–80  $\mu\text{m}$ , which is reasonable considering the average size of a cell is  $\approx 30 \mu\text{m}$  (Figure S6A, Supporting Information). We also considered the pair correlation function (pcf)<sup>[25]</sup> to

complement our analysis. Likewise, the pcf based comparison of the point distributions shows a higher density of cells at distances close to the average cell size under blue light than in the dark, which is another indicator of the blue light dependent cell–cell interactions (Figure S6B, Supporting Information). Yet, Ripley's  $K$ -function and the pcf are sensitive to variations in cell counts/density from one sample to the next, which was not the case for the clustering analysis described above. Therefore, we only compare samples with small differences in cell number using the Ripley's  $K$  and the pcf. From here on we use the clustering analysis as it is more robust against variations in cell density.

Cell–cell interactions are known to be specific in nature and a cell can specifically adhere either to the same type of cell or to that of a different type. We expected to find only heterophilic interactions between CRY2-MDA and CIBN-MDA cells, but not homophilic ones. In order to demonstrate that the blue light-dependent cell–cell interactions are the result of specific binding of CRY2 and CIBN under blue light, we quantified cell clustering in monocultures of CRY2-MDA and CIBN-MDA cells using the same procedure as described above. In these monocultures, cells cluster neither in the dark nor under blue light and have similar clustering parameters as those observed for mixed cultures in the dark (Figure 2A,B). CRY2 has been reported to homodimerize under blue light to some extent.<sup>[26]</sup> However, this interaction does not seem to be strong enough to induce significant cell–cell interactions between CRY2-MDA cells under blue light. Overall, these results show that the cell–cell interactions are only due to the specific heterodimerization of CRY2 and CIBN under blue light. Accordingly, only cells of different types that display these complementary interaction partners will interact with each other under blue light, but not cells of the same type.

A key advantage of the CRY2-CIBN based cell–cell interactions is their reversibility in the dark and the repeated switchability, which reflects the reversible and dynamic nature of native cell–cell interactions. To show that the blue light dependent cell–cell interactions are reversed in the dark, we analyzed the aggregation of the cells in suspension in a light dependent fashion. For this purpose, we co-cultured a 1:1 mixture of CRY2-MDA and CIBN-MDA cells in suspension under constant low agitation (20 rpm) first for 30 min under blue light and then for 30 min in the dark over multiple light/dark cycles. Bright field images taken at each time point allowed visualizing the formation or dissociation of cell aggregates at each stage over three light/dark cycles. We observe that the cells aggregate significantly after each blue light illumination step and that the aggregates dissociate fully after each incubation step in the dark (Figure 3A–F). To quantify the cell aggregation, we defined the objects with an area  $> 5000 \mu\text{m}^2$  as aggregates (at least 15 cells in each aggregate) and computed the percentage of area occupied by clusters and their numbers in the imaged area (Figure 3G; Figure S8, Supporting Information). This analysis shows that both the area covered by large cell aggregates and their overall number is higher under blue light compared to the dark. Hence, we conclude that these blue light dependent cell–cell interactions are both reversible in the dark and can be switched on and off repeatedly.

The dynamics of the blue light dependent cell–cell interactions are another key property that requires investigation at the

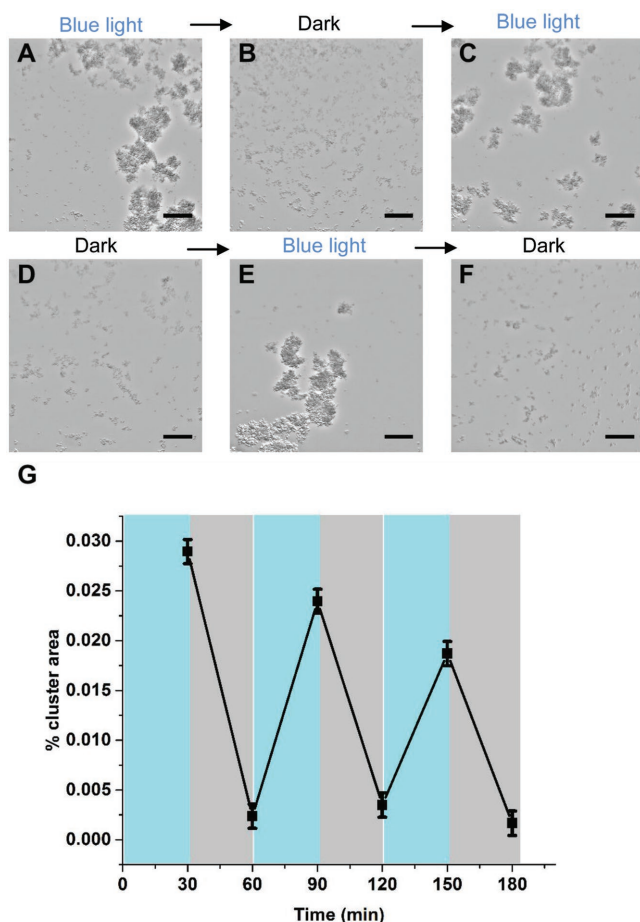


**Figure 3.** Reversible control of cell–cell interactions. A–F) Bright field images of 1:1 suspension coculture of CRY2-MDA and CIBN-MDA in blue light (30 min) and in the dark (30 min) over repeated cycles. The scale bars are 40  $\mu\text{m}$ . G) The change in the percentage cluster area over time in light/dark cycles. Cells formed big clusters under blue light illumination whereas in the dark they dissociated and found to be rather as single cells. The error bars show standard error of the mean ( $n = 6$ ).

level of single cell–cell interactions. In order to determine duration needed for the cells to interact under blue light and dissociate in the dark, we observed single cell–cell interactions live and recorded time-lapse movies. For this purpose, we seeded CRY2-MDA cells on adhesive  $700 \mu\text{m}^2$  circular patterns, so that isolated CRY2-MDA cells grew on an otherwise nonadhesive background. Subsequently, we added CIBN-MDA cells in suspension to these surfaces and examined their interaction with the CRY2-MDA cells first under blue light and then in the dark (Figure 4A; Movie S1, Supporting Information). We further analyzed the distance between the CIBN-MDA and CRY2-MDA cells over time for the light/dark cycle for multiple cells (Figure 4B). When the CIBN-MDA cells are added under blue light illumination the cells quickly bound to the CRY2-MDA cell on the pattern within few minutes resulting in reduced mobility and no measurable distance between the two cells. Further, the two cells remained bound over the 30 min of the blue light illumination. Then, the light was switched off for 20 min and the CIBN-MDA cell separated from the CRY2-MDA cell, gaining mobility. We observed that the CIBN-MDA cell dissociated

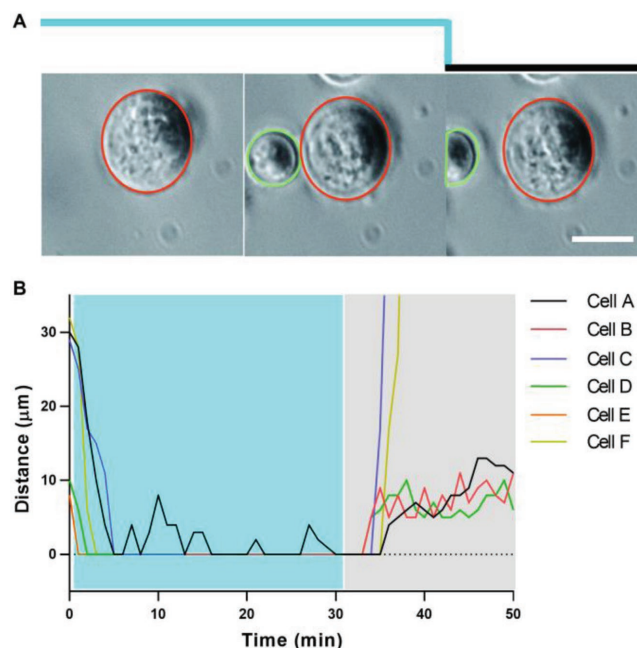


**Figure 4.** Dynamics of light dependent cell–cell interactions. A) Phase contrast images from a time-lapse movie showing the binding of a CIBN-MDA cell to a CRY2-MDA cell under blue light and its dissociation in the dark. The CRY2-MDA cell (red circle) adhered in a circular adhesive pattern with a nonadhesive surrounding. CIBN-MDA (green circle) was added and their interaction was monitored under blue light and in the dark. Scale bar is 25  $\mu\text{m}$ . B) Distance between the CRY2-MDA cells and the CIBN-MDA over time. The distance between the two cells decreases under blue light due to the CRY2/CIBN heterodimerization and increases in the dark due to the CRY2/CIBN dissociation.

from the CRY2-MDA cell within a few minutes once the light was turned off. The proteins CRY2 and CIBN interact with each other under blue light after just a few seconds and dissociate from each other in the dark in about 10 min.<sup>[15a]</sup> Hence, for the formation of the CRY2/CIBN mediated cell–cell interactions the rate limiting step seems to be the cells finding each other as once the two cells were in close proximity the cells were not dissociating from each other. On the other hand, the cells dissociated from each other in the dark in a few minutes; a time range typical for the CRY2/CIBN interaction yet somewhat quicker than the time required for full reversion. Potential reasons for this could be that the switching dynamics are quicker in the extracellular environment than inside the cell or that a minimum number of CRY2/CIBN interaction are required to maintain the cell–cell interactions and when the number of reversed interactions exceeds this limit the cells do not interact anymore.

These blue light switchable cell–cell interactions are suitable to control how cells arrange in tissue culture and produce layered cell structures. Towards this aim, CRY2-MDA and CIBN-MDA cells were used as cellular building blocks to generate a 3D architecture by seeding them layer-by-layer (Figure 5A). First, we seeded CRY2-MDA cells (prestained with a red fluorescent dye) on a glass substrate and grew them to confluency. Then, CIBN-MDA cells (prestained with a green fluorescent dye) were seeded on top of the CRY2-MDA cells and

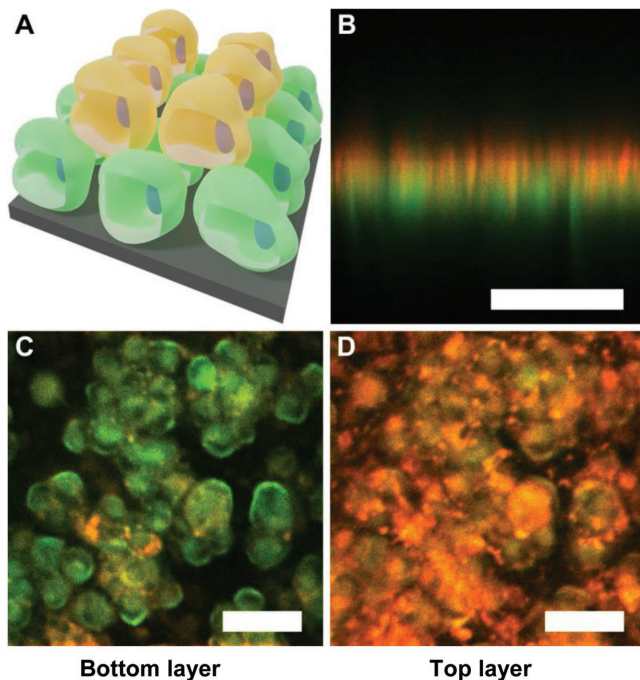


**Figure 5.** Layer by layer 3D architecture. A) Schematic representation of the layered cell structure under blue light. CRY2-MDA cells (green) were grown to confluency, before CIBN-MDA cells (red) are added on top under blue light illumination. CIBN-MDA cells stack on top of the CRY2-MDA cells under blue light illumination resulting in two layers of cells. Confocal images of the B) side view, C) bottom layer, and D) top layer. The scale bars are 50  $\mu\text{m}$ .

were illuminated with blue light for 4h. The confocal images of the coculture showed two layers of cells with red stain CRY2-MDA cells on the bottom and the green stain CIBN-MDA cells on top (Figure 5B–D). Such layered cell structures only formed under blue light illumination and did not form when the CIBN-MDA cells were seeded on top of CRY2-MDA cells in the dark (Figure S9, Supporting Information). Overall, this demonstrates that the blue light dependent cell–cell interactions can be used to form 3D cellular structures from the bottom-up in a controlled manner.

In summary, we have developed blue light switchable cell–cell interactions by using the blue light-dependent heterodimerization of CRY2 and CIBN. We were able to induce interactions between CRY2-MDA and CIBN-MDA cells that express the respective proteins on their surfaces upon blue light illumination and then simply turn them off by switching off the blue light. These photoswitchable cell–cell interactions have the potential to capture key features of native cell–cell interactions in terms of spatiotemporal control, sustainability, dynamics, and reversibility but not cellular signaling associated to cell–cell interaction. Notably, the control with light makes it possible to induce these interactions with unmatched precision in space and time. These interactions are dynamic and reversible, which enables modifying cell–cell interactions over time as observed during biological processes. Additionally, these protein-based photoswitches are well-suited to sustainably control the cell–cell interactions over a long period of time because they are genetically encodable and new proteins are expressed in the cells as they degrade and the

cell divides. The high specificity of the CRY2-CIBN heterodimerization allows us to specifically induce heterophilic interactions but not homophilic ones. Finally, the low intensity blue light that triggers these cell–cell interactions is noninvasive for the cells. These blue light switchable cell–cell interactions can be used to build multicellular architectures, used in scaffold-free bottom-up tissue engineering and also to study biological processes where cell–cell interactions play a pivotal role.

## Supporting Information

Supporting Information is available from the Wiley Online Library or from the author.

## Acknowledgements

S.G.Y. and S.R. contributed equally to this work. The authors acknowledge support by the European Research Council ERC Starting Grant ARTIST (# 757593). The authors would like to thank Prof. J. P. Spatz and Dr. A. E. Cavalcanti-Adam for access to research facilities at the University of Heidelberg, as well as Dr. V. Sakin and Dr. R. Medda for their technical assistance. pCRY2FL(deltaNLS)-mCherryN1 and pCIBN(deltaNLS)-pmGFP were a gift from Chandra Tucker (Addgene plasmid # 26871 and 26867) and pDisplay-AP-CFP-TM was a gift from Alice Ting (Addgene plasmid # 20861).

## Conflict of Interest

The authors declare no conflict of interest.

## Keywords

bottom-up tissue engineering, cell adhesion, cell–cell interactions, photoswitchable proteins, spatiotemporal control

Received: November 20, 2018

Revised: December 14, 2018

Published online:

- [1] a) S. Toda, L. R. Blauch, S. K. Y. Tang, L. Morsut, W. A. Lim, *Science* **2018**, *361*, 156; b) D. L. Elbert, *Curr. Opin. Biotechnol.* **2011**, *22*, 674; c) J. S. Liu, Z. J. Gartner, *Trends Cell Biol.* **2012**, *22*, 683; d) A. C. Wan, *Trends Biotechnol.* **2016**, *34*, 711.
- [2] a) S. Lamouille, J. Xu, R. Derynck, *Nat. Rev. Mol. Cell Biol.* **2014**, *15*, 178; b) B. M. Gumbiner, *Nat. Rev. Mol. Cell Biol.* **2005**, *6*, 622; c) E. Cachat, W. Liu, K. C. Martin, X. Yuan, H. Yin, P. Hohenstein, J. A. Davies, *Sci. Rep.* **2016**, *6*, 20664.
- [3] M.-B. Gema, P. Hector, M. Patricia, O. David, E. Cubillo, V. Santos, J. Palacios, F. P. A. Cano, *Nat. Protoc.* **2009**, *4*, 1591.
- [4] a) D. Duguay, R. A. Foty, M. S. Steinberg, *Dev. Biol.* **2003**, *253*, 309; b) M. S. Steinberg, *Science* **1963**, *141*, 401.
- [5] R. Kalluri, R. A. Weinberg, *J. Clin. Invest.* **2009**, *119*, 1420.
- [6] E. S. Place, N. D. Evans, M. M. Stevens, *Nat. Mater.* **2009**, *8*, 457.
- [7] H. Koo, M. Choi, E. Kim, S. K. Hahn, R. Weissleder, S. H. Yun, *Small* **2015**, *11*, 6458.
- [8] a) D. Dutta, A. Pulsipher, W. Luo, M. N. Yousaf, *J. Am. Chem. Soc.* **2011**, *133*, 8704; b) P. J. O'Brien, W. Luo, D. Rogozhnikov, J. Chen, M. N. Yousaf, *Bioconjugate Chem.* **2015**, *26*, 1939.

- [9] K. Gabrielse, A. Gangar, N. Kumar, J. C. Lee, A. Fegan, J. J. Shen, Q. Li, D. Valleria, C. R. Wagner, *Angew. Chem., Int. Ed* **2014**, *53*, 5112.
- [10] a) Z. J. Gartner, C. R. Bertozzi, *Proc. Natl. Acad. Sci. USA* **2009**, *106*, 4606; b) M. E. Todhunter, N. Y. Jee, A. J. Hughes, M. C. Coyle, A. Cerchiari, J. Farlow, J. C. Garbe, M. A. LaBarge, T. A. Desai, Z. J. Gartner, *Nat. Methods* **2015**, *12*, 975; c) P. Shi, N. Zhao, J. Lai, J. Coyne, E. R. Gaddes, Y. Wang, *Angew. Chem., Int. Ed.* **2018**, *57*, 6800.
- [11] P. A. De Bank, Q. Hou, R. M. Warner, I. V. Wood, B. E. Ali, S. Macneil, D. A. Kendall, B. Kellam, K. M. Shakesheff, L. D. Buttery, *Biotechnol. Bioeng.* **2007**, *97*, 1617.
- [12] J. Wang, B. Cheng, J. Li, Z. Zhang, W. Hong, X. Chen, P. R. Chen, *Angew. Chem., Int. Ed.* **2015**, *54*, 5364.
- [13] W. Luo, A. Pulsipher, D. Dutta, B. M. Lamb, M. N. Yousaf, *Sci. Rep.* **2015**, *4*, 6313.
- [14] a) P. Shi, E. Ju, Z. Yan, N. Gao, J. Wang, J. Hou, Y. Zhang, J. Ren, X. Qu, *Nat. Commun.* **2016**, *7*, 13088; b) P. Shi, E. Ju, J. Wang, Z. Yan, J. Ren, X. Qu, *Mater. Today* **2017**, *20*, 16.
- [15] a) M. J. Kennedy, R. M. Hughes, L. A. Peteya, J. W. Schwartz, M. D. Ehlers, C. L. Tucker, *Nat. Methods* **2010**, *7*, 973; b) A. Taslimi, B. Zoltowski, J. G. Miranda, G. P. Pathak, R. M. Hughes, C. L. Tucker, *Nat. Chem. Biol.* **2016**, *12*, 425.
- [16] a) G. Guglielmi, H. J. Falk, S. De Renzis, *Trends Cell Biol.* **2016**, *26*, 864; b) J. E. Toettcher, C. A. Voigt, O. D. Weiner, W. A. Lim, *Nat. Methods* **2011**, *8*, 35; c) K. Müller, W. Weber, *Mol. BioSyst.* **2013**, *9*, 596.
- [17] L. R. Polstein, C. A. Gersbach, *Nat. Chem. Biol.* **2015**, *11*, 198.
- [18] L. J. Bugaj, A. T. Choksi, C. K. Mesuda, R. S. Kane, D. V. Schaffer, *Nat. Methods* **2013**, *10*, 249.
- [19] a) V. V. Krishnamurthy, J. S. Khamo, W. Mei, A. J. Turgeon, H. M. Ashraf, P. Mondal, D. B. Patel, N. Risner, E. E. Cho, J. Yang, K. Zhang, *Development* **2016**, *143*, 4085; b) O. Idevall-Hagren, E. J. Dickson, B. Hille, D. K. Toomre, P. De Camilli, *Proc. Natl. Acad. Sci. USA* **2012**, *109*, E2316.
- [20] L. Duan, D. Che, K. Zhang, Q. Ong, S. Guo, B. Cui, *Chem. Biol.* **2015**, *22*, 671.
- [21] L. Valon, A. Marin-Llaurado, T. Wyatt, G. Charras, X. Trepat, *Nat. Commun.* **2017**, *8*, 14396.
- [22] S. G. Yüz, J. Ricken, S. V. Wegner, *Adv. Sci.* **2018**, *5*, 1800446.
- [23] M. T. Nieman, R. S. Prudoff, K. R. Johnson, M. J. Wheelock, *J. Cell Biol.* **1999**, *147*, 631.
- [24] B. Ripley, *J. Appl. Probab.* **1976**, *13*, 255.
- [25] D. Stoyan, H. Stoyan, *Fractals, Random Shapes and Point Fields: Methods of Geometrical Statistics*, John Wiley & Sons Inc., Hoboken, NJ, USA **1994**.
- [26] D. L. Che, L. Duan, K. Zhang, B. Cui, *ACS Synth. Biol.* **2015**, *4*, 1124.